JACS
JOURNAL OF THE AMERICAN CHEMICAL SOCIETY

Communication

pubs.acs.org/JACS

Covalent Design for Dye-Sensitized H_2-Evolving Photocathodes Based on a Cobalt Diimine–Dioxime Catalyst

Nicolas Kaeffer,[⊥,†] Julien Massin,[⊥,†] Colette Lebrun,[‡] Olivier Renault,[§] Murielle Chavarot-Kerlidou,[†] and Vincent Artero*[,†]

[†]Laboratory of Chemistry and Biology of Metals, Université Grenoble Alpes, CNRS UMR 5249, Commissariat à l'Energie Atomique et aux Energies Alternatives (CEA), 17 rue des Martyrs, Grenoble 38000, France

[‡]Reconnaissance Ionique et Chimie de Coordination, INAC-SyMMES, Université Grenoble Alpes, Commissariat à l'Energie Atomique et aux Energies Alternatives (CEA), Grenoble 38000, France

[§]Laboratoire d'Electronique et de Technologies de l'Information (LETI), Université Grenoble Alpes, Commissariat à l'Energie Atomique et aux Energies Alternatives (CEA), MINATEC Campus, Grenoble 38054, France

Supporting Information

ABSTRACT: Dye-sensitized photoelectrochemical cells (DS-PECs) for water splitting hold promise for the large-scale storage of solar energy in the form of (solar) fuels, owing to the low cost and ease to process of their constitutive photoelectrode materials. The efficiency of such systems ultimately depends on our capacity to promote unidirectional light-driven electron transfer from the electrode substrate to a catalytic moiety. We report here on the first noble-metal free and covalent dye–catalyst assembly able to achieve photoelectrochemical visible light-driven H_2 evolution in mildly acidic aqueous conditions when grafted onto *p*-type NiO electrode substrate.

Photosynthesis has inspired for many years the development of water splitting dye-sensitized photoelectrochemical cells (DS-PECs) for hydrogen production.[1−3] A key step has been achieved very recently with the report of the first fully operative tandem DS-PEC.[4] In such devices, limitation currently arises from the photocathode performances. Therefore, different architectures based on the cografting[4,5] of catalyst and dye onto nickel oxide (NiO), layer-by-layer[6] or supramolecular linkage of the catalyst to a grafted dye[7] have been investigated. NiO is a *p*-type transparent conducting oxide specifically suitable for fast hole injection from the highest occupied molecular orbital (HOMO) of the excited dye.[8] H_2 evolution requires that the photogenerated electron is efficiently and rapidly transferred to a catalyst. In that perspect, push–pull organic dyes appear as particularly attractive because they combine large absorptivity in the visible spectrum and spatial charge separation in the excited state that limits the undesired recombination reaction from the reduced dye to the NiO electrode.[9,10] The push–pull architecture is also instrumental to foster unilateral electron transfer through direct connection of the acceptor moiety, where the lowest unoccupied molecular orbital (LUMO) is centered and the photogenerated electron located, to the catalyst. We report here the first example of a covalent dye–catalyst molecular assembly integrated in an operative photoelectrode for H_2 evolution (Figure 1).

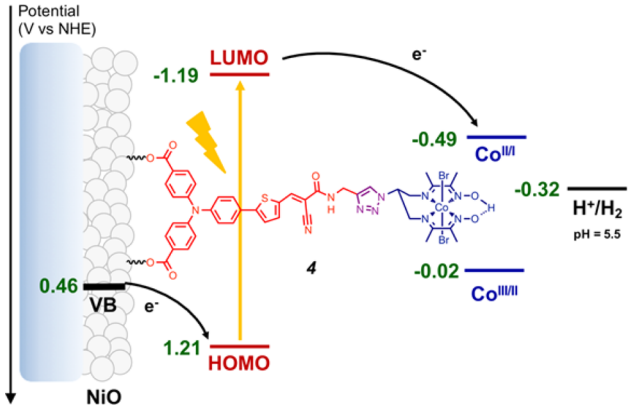

Figure 1. Energy diagram and working principle of the *p*-type photocathode based on **4** at pH 5.5. The NiO valence band edge potential at this pH value was estimated from the 0.37 V vs NHE value determined at pH 7 in ref 17.

We previously reported that, upon grafting on NiO, an easily affordable push–pull dye based on a triarylamine electron-donor part and an ethyl cyanoacetate electron-acceptor part separated by a thiophene unit generates large photocurrents in the presence of an irreversible electron acceptor in mildly acidic aqueous solution (pH 4–5).[11] Cobalt diimine–dioxime complexes are proven catalysts for H_2 evolution at low overvoltage.[12,13] When grafted onto electrode surfaces, they display sustained activity in pH = 4.5 aqueous solution[14] and tolerance to oxygen.[15] These features make them particularly attractive for incorporation into dye-sensitized H_2-evolving photoelectrodes. To prepare a covalent dye–catalyst assembly, we first synthesized a terminal alkyne derivative (**1**, Figure 2) of the above-mentioned dye (Scheme S1). We then used Cu-catalyzed azide–alkyne cycloaddition (Cu-AAC) click chemistry to couple **1** with the copper diimine–dioxime complex $\mathbf{2}_{Cu}$ using conditions previously reported by us.[16] Metal exchange readily occurs through reaction with $CoCl_2$ in acetone; air

Received: June 8, 2016
Published: September 5, 2016

DOI: 10.1021/jacs.6b05865
J. Am. Chem. Soc. 2016, 138, 12308−12311

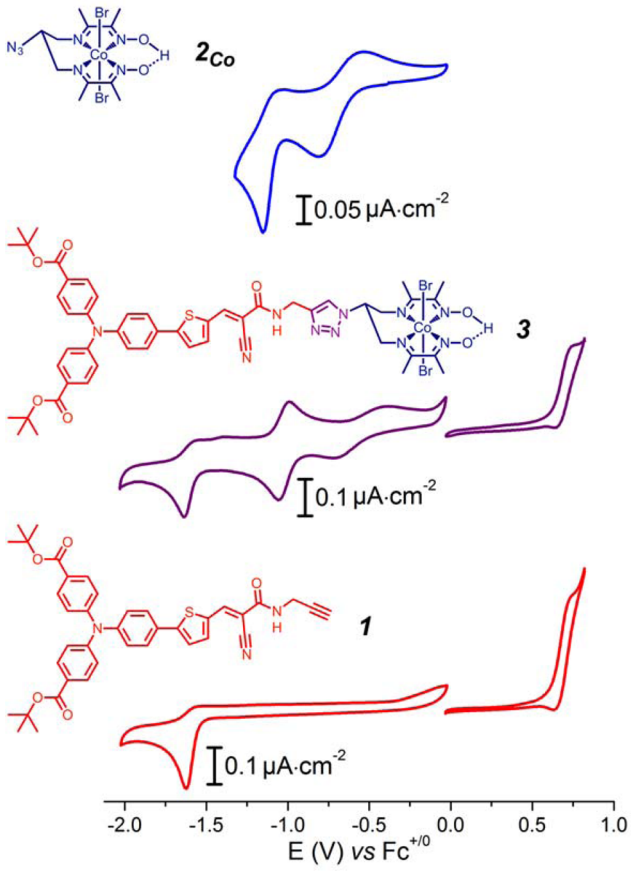

Figure 2. Cyclic voltammograms of **3** (middle) compared with those of $\mathbf{2}_{Co}$ (top) and of the dye precursor **1** (bottom). Measurements were carried out at 100 $mV{\cdot}s^{-1}$ at a glassy carbon electrode (reductive scans) or a Pt electrode (oxidative scans) in DMF (0.1 M nBu$_4$NPF$_6$).

bubbling displaced the equilibrium of this reaction toward the stable and inert Co^{III} derivative.

After purification through silica-gel flash chromatography and precipitation in NaBr-saturated aqueous solution, compound **3** was obtained and its identity was confirmed by ^{1}H and ^{13}C NMR spectroscopy, high resolution electro-spray ionization mass spectrometry (HR ESI-MS) and elemental analysis (see the Supporting Information).

The cyclic voltammogram (CV) of **3** in DMF displays four events (Figure 2, middle). In the anodic regime, a reversible wave is observed at 0.68 V vs $Fc^{+/0}$. We assigned this wave to the oxidation of the triarylamine moiety, by comparison with the electrochemical signature of the dye precursor **1** (Figure 2, bottom).[18] In the cathodic window, the CV of **3** features a first wave at −0.55 V vs $Fc^{+/0}$ and a second reversible wave at −1.02 V vs $Fc^{+/0}$, assigned to the $Co^{III/II}$ and $Co^{II/I}$ couples, respectively, by analogy with the cobalt diimine−dioxime compound $\mathbf{2}_{Co}$ (Figure 2, top). An irreversible cathodic wave monitored at E_p = −1.64 V vs $Fc^{+/0}$ (Figure 2, middle) is assigned to a reduction of the electron accepting group on the dye (Figure 2, bottom).[18,19] The UV−visible spectrum of **3** (Figure S2) corresponds to the sum of the spectra of $\mathbf{2}_{Co}$ and **1**. Compound **3** displays two CT processes characterized by bands at 349 and 431 nm (ε= 33 600 and 31 800 $M^{-1}{\cdot}cm^{-1}$, respectively), the second one corresponding to the HOMO−LUMO transition on the dye unit. The retention of the electrochemical and UV−visible signatures of $\mathbf{2}_{Co}$ and **1** building blocks indicates electronic decoupling of light-harvesting and electrocatalytic components in the covalent dyad **3**. Upon excitation at 430 nm, emission of **3** is observed with maximum intensity at 608 nm (Figure S3). Comparison with the spectrum of **1** reveals 30% fluorescence quenching, suggesting electronic transfer from the excited push−pull moiety to the Co center.

From these data, we could estimate an E_{0-0} value of 2.40 eV leading to a redox potential of −1.72 V vs $Fc^{+/0}$ for the $\mathbf{3}^+/\mathbf{3}^*$ couple (**3*** is the excited state of **3**). Generation of the Co^I state is thus thermodynamically feasible from either **3*** (oxidative quenching) or $\mathbf{3}^-$ (resulting from reductive quenching of **3*** by a sacrificial electron donor or from hole injection from **3*** into NiO valence band), with driving forces of 0.70 and 0.62 eV, respectively.

Photolysis of **3** in CH_3CN in the presence of triethanolamine (TEOA) as electron donor was monitored by UV−visible spectroscopy. Upon irradiation with visible light, the Co^I species builds up within minutes as evidenced by the appearance of the characteristic two-band spectrum with maxima at 595 and 710 nm (Figure 3).[20]

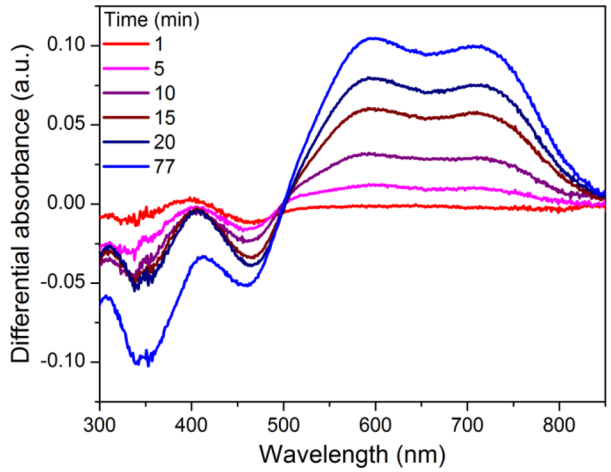

Figure 3. UV−visible monitoring (differential spectra) of the formation of the Co^I derivative of **3** (1.8×10^{-5} M) in CH_3CN/TEOA (90:10 v/v) upon visible-light irradiation.

Reaction of **3** with TFA for 4 h resulted in the quantitative hydrolysis of *tert*-butyl carboxylic esters and isolation of **4** (see the Supporting Information for characterization of **4**). Then, F108-templated[21,22] 1 μm-thick NiO electrodes were prepared and sensitized through soaking in a CH_3CN solution of **4** for 24 h. Chenodeoxycholic acid (CDCA) is a classical coadsorbent utilized in dye-sensitized solar cells (DSSCs) to improve photovoltaic performance.[23,24] We therefore used the typical 4/1 CDCA:dye molar ratio to avoid aggregation of molecules of **4** on the NiO surface.[24] The presence of the Co^{III} centers at the surface of the electrode was confirmed by XPS analysis (Figure S4). From the UV−visible absorption spectra (Figure S5), we estimated 8.2 and 7.2 ± 0.1 $nmol{\cdot}cm^{-2}$ values for surface concentration of **4** immobilized in the absence and in the presence of CDCA, respectively. Such values are similar to those previously measured for **1** on similar electrodes.[11] The presence of CDCA as coadsorbent only slightly impedes the grafting of **4** onto NiO.

The resulting molecular photocathodes were assessed for photoelectrochemical H_2 evolution in a fully aqueous pH 5.5 2-

DOI: 10.1021/jacs.6b05865
J. Am. Chem. Soc. 2016, 138, 12308−12311

(*N*-morpholino)ethanesulfonic acid (MES) buffer. They develop cathodic photocurrents starting from ca. 0.93 V vs RHE (Figure S6) and sustained over the scanned potential range. Two broad processes are observed in the dark around 0.83 and 0.61 V vs RHE and we assigned them to capacitive charging of the NiO film.[25] Chronoamperometric measurements at more negative potentials (0.54, 0.34, and 0.14 V vs RHE) clearly show steady-state cathodic photocurrents (Figure 4, S7 and Table S1). Control experiments on pristine and **1**/CDCA cosensitized NiO electrodes (Figure S7) confirm that the photocurrent is enhanced in the presence of the cobalt diimine−dioxime H_2-evolving catalyst. We therefore ascribe such photocurrents to electron transfer from the NiO valence band to the cobalt diimine−dioxime moiety in **4** via the light-promoted excited state of the photosensitizer unit. Such a process is similar to the one monitored under homogeneous conditions (Figure 3) but with the NiO electrode acting as the electron supplier instead of TEOA. Eventually, the electrons are used by the cobalt diimine−dioxime moiety to reduce protons into H_2. An energy-level diagram of the resulting NiO photocathode sensitized with **4** is shown in Figure 1. The magnitude of the photocurrent proved superior at the most cathodic potential (0.14 V vs RHE) with a current density of ca. −15 $\mu A \cdot cm^{-2}$. We posit that this trend is a result from recombination pathways with the NiO surface slowed down at less positive potentials, as proposed by Hammarström and co-workers.[26] The presence of CDCA as coadsorbent does not modify the initial photocurrent value but significantly improves its stability during continuous irradiation.[27]

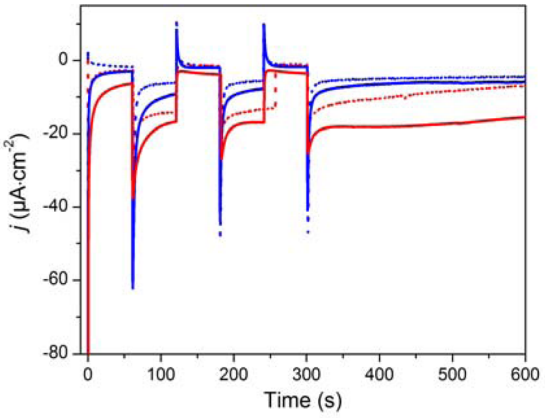

Figure 4. Chopped-light chronoamperometric measurements at **4**-sensitized NiO electrodes poised at 0.14 (red traces) and 0.54 V (blue traces) vs RHE in the absence (dotted) and in the presence of CDCA (plain) under visible-light irradiation (400−800 nm, 65 $mW \cdot cm^{-2}$, 1 sun) in pH 5.5 MES 0.1 M/NaCl 0.1 M supporting electrolyte.

Photoelectrochemical H_2 generation was confirmed by long-term electrolysis at 0.14 V vs RHE under visible-light irradiation (1 sun). During the course of the photoelectrolysis, the magnitude of the photocurrent displayed by **4**/CDCA cosensitized NiO electrodes slowly decreases from 15 to 6 $\mu A \cdot cm^{-2}$ (Table S1). Gas chromatographic analysis of the headspace confirmed the evolution of hydrogen during the chronoamperometric measurements with 8−10% faradaic yields reproducibly and independently measured after 2 and 3 h. Such values are conservative, as they do not take into account H_2 present in solution. Importantly, no H_2 was detected when pristine and **1**/CDCA cosensitized NiO electrodes were measured under similar conditions, despite the passage of 23 and 40 $mC \cdot cm^{-2}$, respectively. To understand this behavior, we recorded the XPS spectra of the photoelectrode at the Ni 2p energy level before and after 2 h of photoelectrochemical H_2 evolution (Figure S8). The $2p_{3/2}$ core region spectrum of the as-prepared electrode contains signals assigned to NiO (853.8 eV and satellite at 862.7 eV) and $Ni(OH)_2$/NiOOH (855.6 eV).[28,29] After photoelectrocatalysis, the principal peak corresponding to NiO shifts to 853.5 eV. This 0.3 eV shift indicates increased amounts of Ni^0 (binding energy of nickel metal $2p_{3/2}$ core region is reported at 852.7−853.1 eV).[28,29] A slight shift of the other peaks is also observed, which can be assigned to a change in the balance between Ni^{III} and Ni^{II} ions as previously observed in a similar context.[30] Formation of metallic nickel and change of redox balance within the NiO film[26,30] provide reasonable explanations for the low faradaic yield for H_2 evolution measured in this work, although we cannot exclude that this also derives from reductive degradation[31] of the dye−catalyst assembly. We also note that the faradaic yields for H_2 evolution reported in previous works describing NiO-based photoelectrodes in aqueous media are generally far from unity,[4,6,7] which suggests that formation of Ni^0 may be quite frequent in this context. Further studies are urgently required to understand this process and develop strategies limiting its extent.

In conclusion, we designed the first covalent and noble metal free dye−catalyst dyad and immobilized it on benchmark F108-templated NiO electrodes. The resulting photocathode based on a cobalt diimine−dioxime catalyst proved functional for light-driven H_2 evolution from fully aqueous solution. We found that cografting of CDCA, a classical coadsorbent in DSSCs but introduced here for the first time in DS-PEC research, has a strong positive influence on the photocurrent stability. In addition, postmortem XPS analysis revealed that competitive reduction of the bulk NiO electrode substrate decreases the faradaic yield for H_2 evolution. These observations open new horizons for gaining deeper understanding of surface confined light-driven electron transfer processes and overcoming the current performance limitations of DS-PEC photocathodes.

■ ASSOCIATED CONTENT

Supporting Information

The Supporting Information is available free of charge on the ACS Publications website at DOI: 10.1021/jacs.6b05865.

Synthesis procedures, experimental details and additional spectroscopic and photoelectrochemical data (PDF)

■ AUTHOR INFORMATION

Corresponding Author

*vincent.artero@cea.fr

Author Contributions

⊥These authors equally contributed to this work.

Notes

The authors declare no competing financial interest.

■ ACKNOWLEDGMENTS

This work was supported by the French National Research Agency (Labex program, ARCANE, ANR-11-LABX-0003-01) and the European Research Council under the European Union's Seventh Framework Program (FP/2007-2013)/ERC Grant Agreement no. 306398. The authors thank J.-F. Lefebvre

DOI: 10.1021/jacs.6b05865
J. Am. Chem. Soc. 2016, 138, 12308−12311

(DPM, Grenoble) and D. Imbert (INAC, Grenoble) for 500 MHz NMR and fluorescence measurements, respectively.

REFERENCES

(1) Ashford, D. L.; Gish, M. K.; Vannucci, A. K.; Brennaman, M. K.; Templeton, J. L.; Papanikolas, J. M.; Meyer, T. J. *Chem. Rev.* **2015**, *115*, 13006−49.
(2) Yu, Z.; Li, F.; Sun, L. *Energy Environ. Sci.* **2015**, *8*, 760−775.
(3) Queyriaux, N.; Kaeffer, N.; Morozan, A.; Chavarot-Kerlidou, M.; Artero, V. *J. Photochem. Photobiol., C* **2015**, *25*, 90−105.
(4) Li, F.; Fan, K.; Xu, B.; Gabrielsson, E.; Daniel, Q.; Li, L.; Sun, L. *J. Am. Chem. Soc.* **2015**, *137*, 9153−9159.
(5) Fan, K.; Li, F.; Wang, L.; Daniel, Q.; Gabrielsson, E.; Sun, L. *Phys. Chem. Chem. Phys.* **2014**, *16*, 25234−25240.
(6) Gross, M. A.; Creissen, C. E.; Orchard, K. L.; Reisner, E. *Chem. Sci.* **2016**, *7*, 5537−5546.
(7) Ji, Z.; He, M.; Huang, Z.; Ozkan, U.; Wu, Y. *J. Am. Chem. Soc.* **2013**, *135*, 11696−11699.
(8) Wood, C. J.; Summers, G. H.; Clark, C. A.; Kaeffer, N.; Braeutigam, M.; Carbone, L. R.; D'Amario, L.; Fan, K.; Farre, Y.; Narbey, S.; Oswald, F.; Stevens, L. A.; Parmenter, C. D. J.; Fay, M. W.; La Torre, A.; Snape, C. E.; Dietzek, B.; Dini, D.; Hammarstrom, L.; Pellegrin, Y.; Odobel, F.; Sun, L.; Artero, V.; Gibson, E. A. *Phys. Chem. Chem. Phys.* **2016**, *18*, 10727−10738.
(9) Qin, P.; Zhu, H. J.; Edvinsson, T.; Boschloo, G.; Hagfeldt, A.; Sun, L. C. *J. Am. Chem. Soc.* **2008**, *130*, 17629−17629.
(10) Mishra, A.; Fischer, M. K. R.; Bauerle, P. *Angew. Chem., Int. Ed.* **2009**, *48*, 2474−2499.
(11) Massin, J.; Bräutigam, M.; Kaeffer, N.; Queyriaux, N.; Field, M. J.; Schacher, F. H.; Popp, J.; Chavarot-Kerlidou, M.; Dietzek, B.; Artero, V. *Interface Focus* **2015**, *5*, 20140083.
(12) Kaeffer, N.; Chavarot-Kerlidou, M.; Artero, V. *Acc. Chem. Res.* **2015**, *48*, 1286−1295.
(13) Jacques, P.-A.; Artero, V.; Pécaut, J.; Fontecave, M. *Proc. Natl. Acad. Sci. U. S. A.* **2009**, *106*, 20627−20632.
(14) Andreiadis, E. S.; Jacques, P. A.; Tran, P. D.; Leyris, A.; Chavarot-Kerlidou, M.; Jousselme, B.; Matheron, M.; Pecaut, J.; Palacin, S.; Fontecave, M.; Artero, V. *Nat. Chem.* **2013**, *5*, 48−53.
(15) Kaeffer, N.; Morozan, A.; Artero, V. *J. Phys. Chem. B* **2015**, *119*, 13707−13.
(16) Queyriaux, N.; Andreiadis, E. S.; Torelli, S.; Pécaut, J.; Veldkamp, B.; Margulies, E.; Wasielewski, M.; Chavarot-Kerlidou, M.; Artero, V. submitted for publication.
(17) Natu, G.; Hasin, P.; Huang, Z.; Ji, Z.; He, M.; Wu, Y. *ACS Appl. Mater. Interfaces* **2012**, *4*, 5922−9.
(18) Ji, Z.; Natu, G.; Huang, Z.; Wu, Y. *Energy Environ. Sci.* **2011**, *4*, 2818−2821.
(19) Yen, Y.-S.; Chen, W.-T.; Hsu, C.-Y.; Chou, H.-H.; Lin, J. T.; Yeh, M.-C. P. *Org. Lett.* **2011**, *13*, 4930−4933.
(20) Smolentsev, G.; Cecconi, B.; Guda, A.; Chavarot-Kerlidou, M.; van Bokhoven, J. A.; Nachtegaal, M.; Artero, V. *Chem. - Eur. J.* **2015**, *21*, 15158−15162.
(21) Li, L.; Gibson, E. A.; Qin, P.; Boschloo, G.; Gorlov, M.; Hagfeldt, A.; Sun, L. C. *Adv. Mater.* **2010**, *22*, 1759−1762.
(22) Sumikura, S.; Mori, S.; Shimizu, S.; Usami, H.; Suzuki, E. *J. Photochem. Photobiol., A* **2008**, *199*, 1−7.
(23) Ito, S.; Miura, H.; Uchida, S.; Takata, M.; Sumioka, K.; Liska, P.; Comte, P.; Pechy, P.; Gratzel, M. *Chem. Commun.* **2008**, 5194−6.
(24) Favereau, L.; Warnan, J.; Pellegrin, Y.; Blart, E.; Boujtita, M.; Jacquemin, D.; Odobel, F. *Chem. Commun.* **2013**, *49*, 8018−20.
(25) Dini, D.; Halpin, Y.; Vos, J. G.; Gibson, E. A. *Coord. Chem. Rev.* **2015**, *304*−*305*, 179−201.
(26) D'Amario, L.; Antila, L. J.; Pettersson Rimgard, B.; Boschloo, G.; Hammarstrom, L. *J. Phys. Chem. Lett.* **2015**, *6*, 779−83.
(27) Addition of CDCA slightly impacts the dark current values.
(28) *Photoelectron Spectroscopy: Principles and Applications*; Hüfner, S., Ed.; Springer: Berlin Heidelberg, 1996.
(29) Renaud, A.; Chavillon, B.; Cario, L.; Pleux, L. L.; Szuwarski, N.; Pellegrin, Y.; Blart, E.; Gautron, E.; Odobel, F.; Jobic, S. *J. Phys. Chem. C* **2013**, *117*, 22478−22483.
(30) Sahara, G.; Abe, R.; Higashi, M.; Morikawa, T.; Maeda, K.; Ueda, Y.; Ishitani, O. *Chem. Commun.* **2015**, *51*, 10722−10725.
(31) Kaeffer, N.; Morozan, A.; Fize, J.; Martinez, E.; Guetaz, L.; Artero, V. *ACS Catal.* **2016**, *6*, 3727−3737.

DOI: 10.1021/jacs.6b05865
J. Am. Chem. Soc. 2016, 138, 12308−12311